POLYTECHNIC JOURNAL

REVEIW ARTICLE

Degradation Mechanisms and Residual Mechanical Properties of Reinforcing Steel Bars Exposed to Natural and Artificial Corrosion – Review & Analysis

Ghafur H. Ahmed[1*], **Ghazi B. Jumaa**[2], **Nasih H. Askandar**[3], **Ahmed S. Ali**[1]

[1] Department of Highway & Bridge Engineering, Technical Engineering College, Erbil Polytechnic University, Erbil, Kurdistan Region, Iraq

[2] Department of Civil Engineering, University of Garmian, Kurdistan Region – Iraq

[3] Department of Civil Engineering, University of Halabja, Kurdistan Region – Iraq

*Corresponding author:
Ghafur H. Ahmed,
Department of Highway &
Bridge Engineering,
Technical Engineering
College, Erbil Polytechnic
University, Erbil, Kurdistan
Region, Iraq.

E-mail:
ghafur.ahmed@epu.edu.iq

ABSTRACT

Reinforcement corrosion is the most problematic phenomenon and one of the main sources for the degradation of structures and infrastructures all across the world, that leads to their premature deterioration before design life has been attained. Therefore, the structural effects of rebar corrosion are crucial in determining the structural performance and residual strength of impaired structures. In the present work, the corrosion initiation mechanisms, corrosion products, corrosion types, corrosion consequences on structural performance and detrimental factors related to corrosion were presented in brief. Moreover, the propagation period and the main consequences on mechanical properties of steel and concrete are analyzed. Analyses of the available statistical data collected from literature were performed for 443 specimens. The findings are further interpreted from structural point of view, and deterioration equations for the mechanical properties of the corroded reinforcements are developed. The relations are well analyzed, leading to the definition of decay equation for yielding and ultimate stresses, and ultimate strain. It was found that the mass loss of 1% due to the rebar corrosion can cause the strength loss of 1.34%, 1.30%, and 3.54% respectively for yield strength, ultimate strength, and elongation. The suggested formulas can be applied in analytical and numerical structural applications.

Keywords: Reinforcement bars; mechanical properties; accelerated corrosion; uniform corrosion; pitting corrosion.

INTRODUCTION

In recent years, corrosion phenomena of the reinforcing steel have received extreme attention because it is among the primary materials that result in mechanical damage to reinforced concrete (RC), which is the most commonly employed building material. The corrosion phenomena of reinforcement bars embedded through concrete considered in a way or another as an extreme substantial factor leading to the event of deterioration of any structures built out of concrete and thus, bring out severe damage. Concrete reinforcing bars protected by ordinarily a passive film established through alkaline environment (*pH* of 13.5) due to cement hydration products.

Yet, the passive film could be ruined via the entree of aggressive ions like carbon dioxide and chloride. Due to the variety of extrinsic environments, non-homogeneous properties of these two; passive film and concrete cover, metallurgical and compositional non-uniformity of steel reinforcement, corrosion phenomena in implementation are overwhelmingly seemed to be non-uniformly disseminate along the length of a steel bar. Corrosion process is renowned in reinforced concrete structures by brown patches of rust that protrude on the concrete surface and/or cracked concrete cover. Direct consequences of the corrosion practicability are: (i) reduction of rebar area and ductility, and (ii) volume expansion of corrosion products (Garcia et al., 2019; Jiang et al., 2020; Garcia et al., 2021;

Koulouris & Apostolopoulos, 2021).

The incredibly desirable prerequisite for durability cannot constantly accomplished practically, owing to that corrosion of rebar in concrete recently been repeatedly encountered as source of deterioration in numerous counts of RC structures. The surface of the steel develops a thin, compact, and stable passive oxide coating owing to the concrete's high alkalinity. There are two aspects of oxygen in concrete, according to research; gaseous oxygen can pass into the water-unsaturated pores, whereas dissolved oxygen been imparted within pore liquid water. The corrosion process basically causes a decrease in the reinforcing steel's ductility and strength, as well as a reduction in the cross-section. Consequently, both the bearing and dissipative capacities of the structural component are diminished. Two dissimilar corrosion morphologies, localized or uniform, can occur, primarily due to different process of degradation: carbonation decay, associated with CO_2 ions passing within the concrete core, in addition chloride attack, owing to existence of the chlorides in the environment (Ahmad, 2003; Balestra et al. 2019; Diaz et al. 2020; Brito et al. 2021). Throughout carbonation and chloride phenomena mechanical properties of steel significantly decreased. Decline of the reinforcement area, strength, and ductility straight influences the stiffness of the structure, the like hood for force and moment redistribution, and limits the load-carrying capacity of RC structures. Rust volume expansion could result in cracks and spalls in the nearby concrete. Concrete that has cracks impacts both the actual shear and anchoring capacities as well as the long-term load carrying ability. Enormous resources being spent these days to work out the deterioration issues of current RC structures to assure their safety and sustainability. It had been claimed that over $20 billion are required annually in the USA for the maintenance and renovation of highway structures, and over £600 million prerequisite per annum in the UK for repairing road as well as bridges. In the USA alone, for instance, it is estimated that $1.8 trillion need be invested for upcoming 20 years to sustain roads and bridges current status. Additionally, $627 billion are necessary throughout both at once frame to raise these infrastructure systems' quality to necessary levels. Thus, corrosion of the reinforcing steel is a primary contributing factor in degradation issues. It is estimated that the worldwide maintenance and repair costs for corrosion of RC facilities can reach $100B/yr. (Michel et al. 2016; Hu et al. 2019).
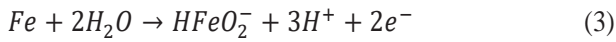
When considering the residual lifetime of the corroded structures, it is necessary to predefine the aggressiveness of the environment where the structure has to be built, and the time dependent mechanical properties of the corroded rebar embedded in concrete. Hence, it is equivalent outlining equations of steel degradation regarding mechanical characteristics of the corroded rebar. Numerous investigations have inscribed both case formation and stability regarding passive film in solutions simulating the concrete pore environment. Yet, the long-term behavior is rarely included in studies, that which reinforced concrete specimens need to be taken into account. The primary unknowns relate to determining the residual area of reinforcing bars exposed to pitting corrosion, early brittle failure mechanisms, or the impact of bond deterioration on the overall structural response of RC beams. Additionally, novel studies address the fragile behavior of external pits and internal defects. Some researchers have started these days to study pit morphology. They discovered that pits grow up in a rapid way through depth than in width, regardless of irregular pits are less frequent, they are utmost severe, due to the fact that they are the deepest ones (Fernandez et al., 2015; Finozzi et al., 2018). Regarding the present work, the corrosion initiation mechanisms, time-dependent states of reinforcement corrosion, corrosion products, corrosion types, corrosion morphology, cleaning of the corrosion products, mechanisms and differences between chloride induced and carbonation induced, natural and accelerated corrosions were explained. Corrosion consequences on structural performance and detrimental factors related to corrosion were briefly discussed. Moreover, the corrosion induced crack propagation period as well as the major impact on mechanical properties are analyzed for steel as well as concrete. Analyses of the statistical data collected from literature were performed for 443 specimens. The findings are further interpreted structurally, and degradation equations are established regarding mechanical characteristics of the corroded reinforcements. Applications of analytical and numerical structural analysis can benefit from the proposed formulations.

CORROSION MECHANISMS OF STEEL EMBEDDED IN CONCRETE

Traditional steel reinforcement often corrodes due to electrochemical reactions like oxidation reaction at the anode (electron loss), in addition a reduction of reaction at the cathode (gain of electron). A brief transient in the electric charges might result from coupled anodic and cathodic reactions. As per Faraday's electrolysis laws, the quantity of material that interacts or is released is proportional to a range of electric charges traveling through it. The result of these electrical charges is oxidation or corrosion of steel. (Tang, 2019). Process of corrosion is stated to be identical to that of flash batteries action. Corroding steel rebar surfaces behave as a combined electrode, with anodes and cathodes electrically linked to the steel's body, where coupled anodic and cathodic reactions occur (Fig.1a). Half-cell reactions are commonly used to identify reactions that occur at the anode and cathode. The anodic reaction leading to metal dissolution or loss, however the cathodic reaction outcomes the dissolved oxygen decreases and the creation of hydroxyl ions (Eid et al. 2020). Possible anodic reactions for steel embedded in concrete are represented by equations Eq.1–4 below, which depend on pH level of the interstitial electrolyte, the occurrence of aggressive anions, as well as the availability of a suitable electrochemical potential at the rebar surface of

aggressive anions, and the availability of a proper electrochemical potential at the rebar surface:

$$3Fe + 4H_2O \rightarrow Fe_3O_4 + 8H^+ + 8e^- \qquad (1)$$

$$2Fe + 3H_2O \rightarrow Fe_2O_3 + 6H^+ + 6e^- \qquad (2)$$

$$Fe + 2H_2O \rightarrow HFeO_2^- + 3H^+ + 2e^- \qquad (3)$$

$$Fe \rightarrow Fe^{2+} + 2e^- \qquad (4)$$

There must be O_2 and a certain pH level close to the steel surface for cathodic reactions to occur, and one likely responses are as in Eq.5 – 6:

$$2H_2O + O_2 + 4e^- \rightarrow 4OH^- \qquad (5)$$

$$2H^+ + 2e^- \rightarrow H_2 \qquad (6)$$

TIME-DEPENDENT STATES OF REINFORCEMENT CORROSION

It is possible to anticipate that the degree of steel corrosion in concrete will alter over time. De-passivation, propagation, and final state are the three separate steps of the corrosion process, as illustrated in (Fig.1b). The lack of the oxide (passive) layer that forms on the rebar owing to the elevated alkalinity of concrete is referred to as de-passivation. De-passivation requires an inception period (t_p), that is the timeframe between construction and the start of corrosion. The propagation phase begins at the time of de-passivation (t_p), progressing into final state, in which it arrives at a critical time (t_{cr}), as a consequence of corrosion, the concrete cover may spall or crack. Throughout the propagation period, i.e., corrosion period (t_{cor}), the rebar corrosion is ordinarily presumed being in a steady state, as specified by a straight line (Fig.1b).
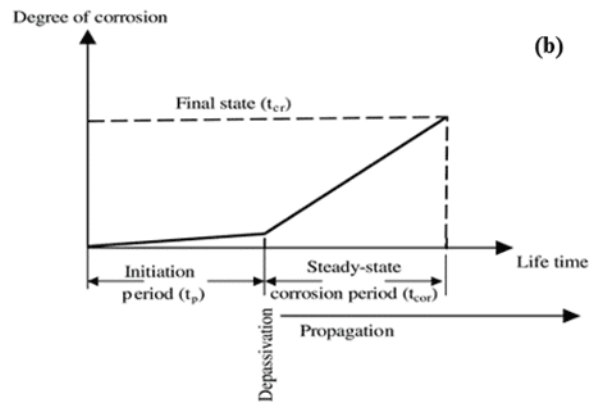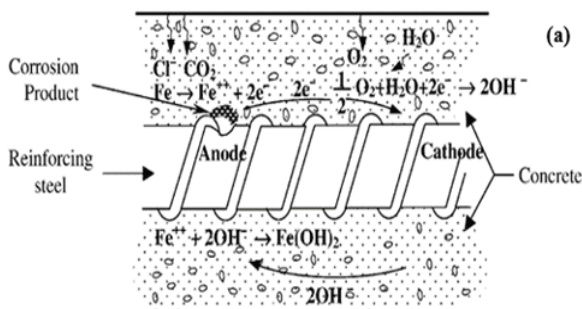

Fig.1. (a) Schematic illustration of the corrosion of rebar embedded in concrete (b) The stages of the rebar corrosion (Ahmad, 2003).

The critical time can be expressed as: $t_{cr} = t_p + t_{cor}$. Subsequently, the critical time might be equivalent to the service life. The de-passivation time (t_p), whenever proportion of free chloride ions added to the concrete during makeup by any mechanism is taken as zero, discovered to be beyond the rebar corrosion threshold magnitude (Ahmad, 2003).

CORROSION PRODUCTS

After corrosion begins, the corrosion products (iron oxides), which have a lower density, occupy a significantly greater volume than the initial iron. Accordingly, corrosion advances, corrosion products cumulate in interfacial transition zone (ITZ) and exert expansion pressure on the concrete around it (Fig.2). The pressure rises up to the point where cracks develop and spread. Depending on a variety of conditions, including pH levels of the pore solution, the presence of moisture as well as oxygen, the ability of aggressive agents, etc., the development of corrosion complex stoichiometry possibly led the iron to expand 4-6 times its initial volume. In comparison to the original iron metal, Table 1 summarizes the characteristic physical attributes of the common corrosion products. broadly, it is believed that two types of corrosion predominate: ferrous hydroxide Fe (OH)$_2$ and hydrated red rust, ferric hydroxide Fe (OH)$_3$. For instance, the volume of the corrosion product of ferrous hydroxide is four times more than that of burnt ferrite. This causes internal tension, which leads to delamination and spalling in the end. External loading may further speed the failure process (Chen & Mahadevan, 2008). The corrosion process of reinforced concrete is sorted into three phases: (i) initially free expansion of rust, rebar/concrete interface voids are filled by steel corrosion products; (ii) tensile stress amid concrete cover, wherein the concrete cover begins to crack; in addition, (iii) cracking in the concrete covering, wherein the crack is still brimming with rust products (Xu & Jin, 2018; Chen, 2022). The reinforcements will be immersed in a 12 % hydrochloric acid solution for almost 15

minutes before being rinsed in water and neutralized using lime water. Finally, for four hours, the reinforcements must be rinsed and dried (Fig.2c) (Gao et al., 2019).

CORROSION MORPHOLOGY

Non-uniform corrosion is defined by the greatest depth of corrosion and the biggest area of corrosion of deteriorated reinforcements. Current models for predicting reinforcement pitting characteristics were largely concerned with the impacts of the concrete cover, reinforcement diameter, and corrosion current density, but gave little consideration to the effects of chloride concentrations on corrosion at the reinforcement surface. This may have an influence on beam and slab shear and flexural strength, in addition to seismic activity and axial strength of RC columns and walls. According to research, in an accelerated corrosion process, uniform corrosion could happen -
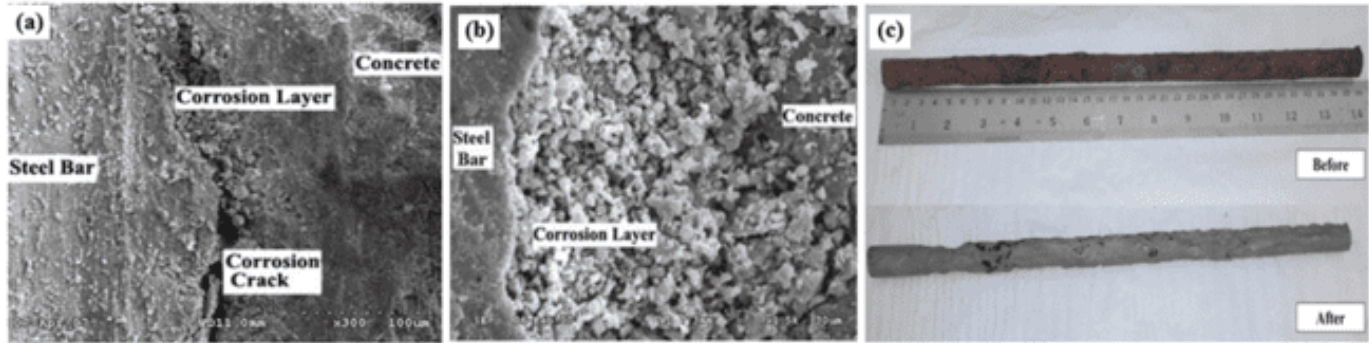

Fig.2. Microstructure of corrosion layer (a) 1500x, (b) cracking on the interface (Yuan et al. 2009), (c) Specimens before and after cleaning process to remove corrosion products (Balestra, 2016).

Table 1 Characteristic relative volume ratios of corrosion products

Corrosion product	Fe	FeO	Fe2O3	Fe3O4	Fe(OH)2	Fe(OH)3	Fe(OH)3.3H2O
Relative volume ratio	1.0	1.7	2.1	2.0	3.6	4.0	6.2
Molecular weight	56	72	160	232	90	107	161
Density (x 103 kg/m3)	7.85	5.93	10.67	16.24	3.50	3.75	3.64
Specific volume (g/cm3)	0.127	0.169	0.094	0.062	0.286	0.267	0.275
Relative specific volume	1.00	1.32	0.74	0.48	2.24	2.09	2.16

continually, but non-uniform corrosion occurs in the natural environment (Fig.3). Under continuous stresses, both natural and accelerated, uniform and non-uniform corrosion can happen simultaneously. Furthermore, chloride corrosion of concrete reinforcements in the tension zone is worse than corrosion in the compression zone (Abdelatif et al., 2018). Corrosion was determined to have a stronger influence over tensile characteristics of plain rounded bars than deformed (ribbed) bars, and at the same way it has a greater impact on the smaller size bars than larger ones for the same corrosion mass loss.

MICROSTRUCTURE CONSIDERATIONS

A reinforcing steel bar is composed of several layers (martensite-bainite-pearlite, Fig.4), all with its unique stress-strain law. The martensite cortex is still more strong with lower ductile than that at inner bainite layer, which is also perhaps weaker than the pearlitic core. The volumetric proportion between these layers determines the overall reinforcement constitutive law, and its mechanical properties. The ratio may vary greatly within same corrosion level in the situation of localized corrosion or relatively marginally when there is uniform corrosion. Obviously, the two morphologies might overlap in practice, as well as when pitting corrosion develops, a uniform drop in the section may be noticed locally. The mass loss in the investigated experimental campaign is closely connected to the progressive reduction of the martensitic layer, which ensures hardness and strength, in addition subsequently a lessening of mechanical properties of reinforcement (Bautista et al., 2019; Soleimani et al., 2020).

Fig.3. Longitudinal direction of reinforcement bars showing uniform corrosion and pitting corrosion (Finozzi et al. 2018; Ahmed, 2022).
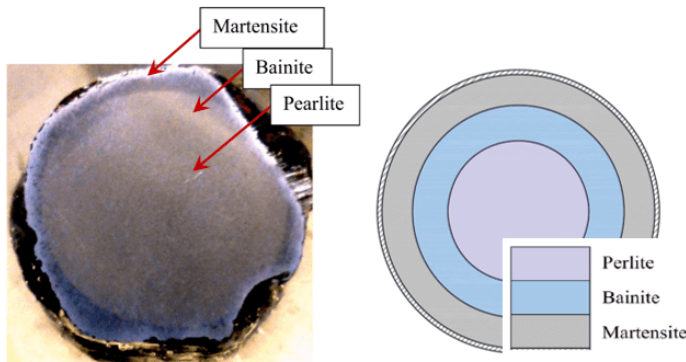

Fig.4. Metallographic depiction of reinforced bar with the indication of the layers (Imperatore et al. 2017).

CORROSION TYPES IN REINFORCING STEEL

The application of reinforcement bars in reinforced concrete has been discovered at the end of the nineteenth century. Thousands of investigations on the corrosion of reinforcing steel bars have been conducted since that time. The two most likely mutual sources of steel bar corrosion are chloride attack as well as concrete carbonation, which may have existed in the concrete constituent as from the very start or are inserted by intrusion into the concrete over its service life. The latter is much prevalent also it is commonly brought up by de-icing salt, airborne salt, and/or chloride-contaminated aggregate, latest one apparently due to carbon dioxide from the air and/or water (Ahmed, 2015; Ou et al., 2016).

Chloride-induced Corrosion

A magnificent passive layer of oxide preserves concrete's steel reinforcing bars from oxygen and moisture, which might lead to corrosion and rust. Only at high *pH* levels (higher than 12) can this passive layer be maintained or with a chloride ion concentration below the corrosion threshold. De-passivation, or the removal of the protective layer occurs whenever chloride ions infiltrate to concrete and builds up to such critical level on the steel's surface (Fig.5a). Chloride-induced corrosion (Eq.7–8) primarily depends on three variables: the critical chloride level, the diffusion coefficient, as well as surface chloride concentration. Under chloride corrosion attack, the service life of concrete structures is further evaluative to cover depth rather than diffusion coefficient as well as to chloride concentration than to the critical chloride level. When water or oxygen are scarce, the corrosion process will sluggish and maybe cease. A lack of water in dry concrete also slows corrosion action, as does extremely high humidity, which both slows the passage of oxygen into corrosion area, as well as reinforcing corrosion (Wang et al. 2010; Zhang et al., 2014).

$$Fe^{++} + 2Cl^- \rightarrow FeCl_2 \qquad (7)$$

$$FeCl_2 + 2H_2O \rightarrow Fe(OH)_2 + 2HCl \qquad (8)$$
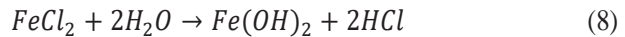
Once the corrosion process begins, propagation occurs in three steps: a preliminary stage when corrosion products perforate the porous network about the steel rebar and fill the steel/concrete interface; the second step is defined by stress commencement because the corrosion accommodation zone has been entirely brimming with rust products that are beginning to impose stress; and last stage marked by crack development when stress approaches the steel's tensile strength. As a result, expanding stress develops in the concrete, resulting in cracking, spalling, or delamination of the cover. At the end of the propagation stage, corrosion reduces rebar cross-section and induces bond loss between concrete and steel (Jones et al., 2015). Structures with already having dry joints such those in segmental construction, or weakly bonded 3D printed layer-by-layer concrete elements could be more vulnerable to such attacks, as the chloride can easily transfer through the joints (Ahmed & Aziz, 2019, Ahmed et al., 2022). Broadly, the concentration of chloride corrosion is detected when chlorides surpass 0.4 % by cement weight (for chlorides cast into concrete) or 0.2 % (for chlorides diffused in concrete). The rate of corrosion propagation influenced by the existence of oxygen and water near the cathode. However, significant pitting has been observed even at low O_2 levels. It can be explained by the possibility that whereas the equivalent cathodic sites may be dispersed over a large area, the anodic sites may be confined. This prevents the corrosion product from precipitating, and because there are localized, highly active anodic sites, severe pitting corrosion occurs without prior notice and leaves noticeable evidence on the nearby concrete (Shekhar et al., 2018).

Carbonation-induced corrosion

Tricalcium silicate (3CaO.SiO$_2$), dicalcium silicate (2CaO.SiO$_2$), tricalcium aluminate (3CaO.Al2O$_3$), and calcium aluminoferrite (4CaO.Al2O$_3$.Fe2O$_3$) are common components of cement in concrete. These are frequently abbreviated as C$_3$S, C$_2$S, C$_3$A, and C4AF. Whenever cement combines water, the hydration procedure creates crystalline calcium hydroxide, or portlandite Ca (OH)$_2$ (CH), as well as a gel of hydrated CaO.SiO$_2$nH$_2$O (CSH) and other heat-evolving compounds. Carbonation in the concrete is primarily produced by the entry of atmospheric CO$_2$, particularly when relative humidity levels are 50-70%. Whenever pH level of concrete falls below a threshold level, the carbonation process begins, resulting in corrosion, cracking, and spalling, as illustrated (Fig.5b). Carbonate is formed when carbon dioxide combines with CH and CSH, which lowers the *pH* magnitude of the concrete and removes the passive layer. Carbonation causes shrinkage and a drop in *pH* magnitude to a critical level, which causes corrosion to begin. Carbonation is related to the water/cement ratio and occurs in proportion to the square root of time. (Wang et al., 2010). Carbonates in marine environments

can come from either the sea water or atmosphere. Concrete carbonation is a neutralizing reaction that occurs between carbon dioxide absorbed from the surrounding atmosphere and alkaline hydration products (e.g., calcium hydroxide) for concrete originating from air. Carbonation of concrete is induced by a metathesis event between the bicarbonate ion (HCO_3^-) in seawater and alkaline hydration products, as detailed through Eqs.9–12 (Hu et al. 2018).

(1) Dissolution of CO_2 in the sea water (Eq.9), and in the fresh water (Eq.10).

$$CO_2 + H_2O + CO_3^- \rightarrow 2HCO_3^- \qquad (9)$$

$$CO_2 + H_2O \rightarrow H_2CO_3 \qquad (10)$$
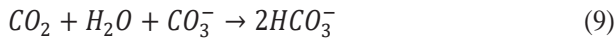
(2) Metathesis reaction between HCO_3^- (with concentration of 140 mg/L in seawater) and OH^- (Eq.11), and precipitation reaction in between CO_3^- and the calcium ion Ca^{2+} (Eq.12).

$$HCO_3^- + OH^- \rightarrow CO_3^- + H_2O \qquad (11)$$

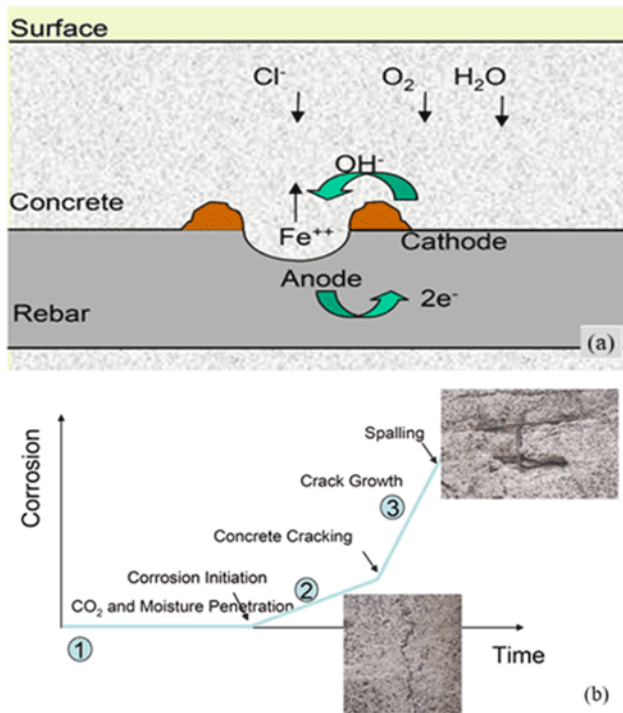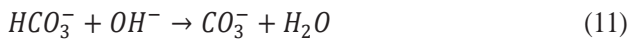$$CO_3^- + Ca^{2+} \rightarrow CaCO_3 \downarrow \qquad (12)$$

Fig.5. (a) an electrochemical cell induced by chloride penetration, (b) the three stages in carbonation-induced corrosion (Wang et al. 2010).

NATURAL AND ARTIFICIAL CORROSION

Preferably, testing should be carried out on naturally corroded bars. Natural corrosion of steel, on the other hand, is a rather gradual process, and it is sometimes hard to remove corroded bars from still-in-use structures. Because alkalinity of concrete, corrosion takes a longer time to commence even when exposed to very corrosive conditions. Because of the extensive time periods necessary to duplicate reinforcement corrosion in laboratories, accelerated corrosion test procedures have been developed. With both bare and embedded bars in concrete, artificial corrosion methods implicate cyclic wetting and drying, salt spray, and the impressed-current approach. The impressed voltage technique is one of many accelerated corrosion test procedures that are well-known for being efficient and fast, lowering corrosion start or de-passivation time from years to days (Table 2). The impressed-current approach utilized in the previous studies with corrosion current density varied from 0.01 to 2.4 mA/cm^2, whilst in natural corrosion, the density consistently varies from 0.001 to 0.003 mA/cm^2. It is currently unclear how such variations in the current density affect the tensile properties of corroded steel bars. According to studies, concrete bars implanted in artificial corrosion developed corrosion patterns that had more pitting than bare bars did. With increasing corrosion mass, each of strength as well as deformation capacity of naturally as well as artificially corroded bars tended to decline. In contrast to strength, the trend for deformation capacity was less obvious. This is due to the fact that the deformation capacity is also connected to shape changes along the bar, whereas the strength capacity was primarily tied to the minimal cross-sectional area (Ou et al., 2016; Uthaman et al., 2019). In comparison to steel samples in direct contact with the same corrosive medium, the degradation of steel bars buried in concrete resulted in much extensive pitting corrosion in terms of pit depth with the same average mass loss. When comparing the embedded and bare bars (Fig.6) with the same amount of mass loss (2.4%), the yield strength and the ultimate strain were 3.1 and 3.2 times higher in embedded bars, respectively. The ultimate strain values of naturally corroded bars were lower than artificially corroded ones, whereas both of yield and ultimate stresses were similar. This demonstrates that, as compared to naturally corroded, the allocation of sectional areas in artificially corroded bars was more irregular (Apostolopoulos et al. 2013).

Table 2 Illustration of advantages and disadvantages of naturally and artificially corroded rebar tests

Type	Advantages	Disadvantages
Natural corrosion	Corrosion process is that exactly happening under natural exposure.	Unacceptable period required for a high corrosion level that exceeding years or decades.

|			
	Corrosion characteristics are that under natural environment and of 100% accuracy.		Corrosion level along the rebar embedded in concrete cannot be totally observed.
	Deterioration results can be useful for similar projects in similar environments.		Corrosion environment and process are uncontrollable.
Artificial corrosion	Corrosion levels can be controlled precisely.		Corrosion process differs from that under natural environment.
	By adjusting the current density, the corrosion time needed to achieve the desired corrosion rate may be made acceptable and flexible.		Corrosion characteristics of the rebar differ from those under natural environment, no clear relations have been defined yet.
	The corrosion process is simple to implement and inexpensive.		Different test setup, test procedure and measurement technics lead to controversial results by researchers.
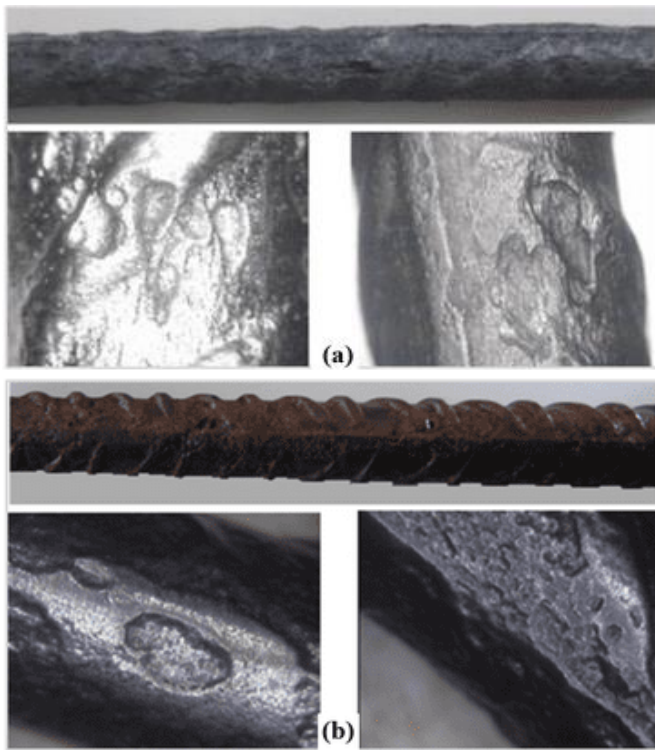
Fig.6. Corrosion effects on surfaces of (a) embedded specimens in concrete exposed to salt spray for 1 year, and (b) bare bars exposed to salt spray for 20 days (Apostolopoulos et al. 2013).

FACTORS AFFECTING CORROSION OF STEEL IN CONCRETE

Existence of oxygen as well as moisture at rebar level supports the propagation of corrosion. Moisture meets the corrosion cell's electrolytic need, and moisture and oxygen work together to generate additional OH^-, resulting in a rise of rust components, i.e., $Fe(OH)_2$. Cathodic reaction progress is impacted by oxygen, and cathodic polarization prevents corrosion from advancing in the lack of adequate oxygen, even in a de-passivation state. The relative humidity at most influence the carbonation of concrete. Range from 50 to100% of RH, the raise of environmental relative humidity contracting carbonation of concrete. A temperature increase could have two effects.: (i) the electrode reaction levels in general rises, and (ii) the oxygen solubility dropped down as a result of which the rate of corrosion is reduced. Due to their propensity to lower the pH of the concrete, carbonation and other acidic gases, as in SO_2 and NO_2, have an impact. The fall in the *pH* to 9.5 as a result of which reinforcing corrosion begins, loss of passivity of concrete at *pH* of 8.0, and catastrophic corrosion for *pH* values below 7. Aggressive anions, primarily chloride ions, entering the concrete from the ingredients or entering from the outside environment and reaching the rebar level. In addition to being chemically bound with hydration products like C_3A or C_4AF and loosely bound with CSH gel, chloride can also be found in concrete as free or water-soluble bound chloride, this is the free chloride ion concentration (Cl^-) in the concrete's pore solution, and acid soluble chloride. It is commonly acknowledged that the corrosion process is only affected by free chloride ions. The recommended chloride content by weight of cement is limited to be 0.15%. In three ways Bacterial activity has been discovered to be effective: (i) corrosion-causing differential aeration cells may grow with the help of aerobic microorganisms, (ii) in oxygen-deficient environments like concrete sewers, anaerobic bacteria produce iron sulfides, which makes corrosion possible even when there is no oxygen, and (iii) by causing the cementitious components to disintegrate, bacteria reduce the amount of cover. (Firodiya et al. 2015). In additions to the mentioned external factors, many internal factors can cause or accelerate the rebar corrosion. Because of the reaction between C_3A and C_4AF in concrete, the cement within concrete protects the reinforcing steel from corrosion by absorbing a sizable amount of chlorides, and by maintaining a high *pH* (12.5–13) since the hydration product contains $Ca(OH)_2$ and other alkaline elements. It has been discovered that using blended cement, like micro-silica blended high-C_3A cement, makes it more resistant to both sulfate attack and chloride corrosion. One of the most common sources of chloride in concrete is the addition of calcium chloride, a popular chemical used to accelerate hydration. Chlorides are another component of several water lowering admixtures. It may be harmful to mix and cure water that is either excessively chloride-contaminated or extremely acidified. When the RC structures submerged into an aggressive solution, the corrosion of the rebar is influenced by the permeability of the concrete as a function of the water-to-cement (w/c) ratio. The depth of penetration of a specified chloride threshold value rising when the w/c ratio increases. Carbonation depth is linearly rising in conjunction with increased value of the w/c ratio. Serious corrosion issues are

brought on by aggregates containing impurities or chloride salts, especially when seawater is involved. Cover depth significantly affects corrosion caused by chloride or carbonation penetration. Differential corrosion cells are produced as a result of changes in the chemical makeup as well as structural makeup of the reinforcing steel as well as the existence of stress in the reinforcement, both cyclic and static (Ahmad, 2003; Ahmed, 2022).

CONSEQUENCE OF CORROSION ON STRUCTURAL BEHAVIOR

Steel reinforcement corrosion is among the most severe threats to RC structures nowadays. Multiple mutual consequences occur when reinforcements in reinforced concrete structures deteriorate (Fig.7): degradation of the steel-concrete bond; steel cross-section decrease, also concrete cover longitudinally cracking because of expansive corrosion agents. The load-bearing capacity in addition, service life of reinforced concrete structures are significantly decreased as a result of these impacts. Studies show that cracks hasten the onset of corrosion by giving aggressive agents preferential paths (gaseous, liquid, and ionic). Particularly for structures in coastal areas, corrosion of reinforcement will result in deteriorated joint performance under seismic events (Lin et al., 2017; Zhang et al., 2018; Zhang et al., 2020). Structures are damaged by steel rebar corrosion mostly due to: (i) decrease in rebar mechanical characteristics (ii) decrease in rebar cross-sectional area; and (iii) weakening in concrete-rebar bond. The rust products exert a recumbent stress on the adjacent concrete whose tensile strength is commonly low. The value of reinforcement corrosion has a considerable effect on deformational behavior, flexural strength, bond strength, ductility, and style of failure of the RC structures. Correspondingly, among the most crucial factors in forecasting the usable service life of corroding RC structures is the degree of corrosion (Uygunogu & Gunes, 2015; Sola et al. 2019).

RELATIONSHIP OF CORROSION AND BAR

MECHANICAL PROPERTIES

In the relevant standards, the capability of a steel bar regarding mechanical performance is assumed to remain constant over the whole lifespan of a reinforced concrete structure, whereas corrosion can cause drastic changes in the rebar mechanical properties.

Reduction of cross-sectional area and mass loss

Corrosion causes rust accumulation by lowering the bars' cross-sectional area, resulting in spalling as well as cracking of the concrete cover over the bars. influencing the long-term strength as well as serviceability of the structural system. In the probabilistic forecast of the enduring service life of RC Structures undergoing corrosion, the quantification of the mutability of corrosion rates of reinforcing bars is crucial. Micrograph analysis revealed that smaller-diameter steel rebar exhibited worse deteriorations than larger-diameter rebar. On the surface of Ø12 rebar, larger cavities observed than that on Ø16 rebar surface. As a result, there was a connection between the surface pitting of steel rebar and the loss of cross-section, which strongly shows that an increase in surface pitting was associated with a decrease in the cross-section of steel rebar. According to research, the flexural strength findings of beams are relatively similar at the beginning of corrosion, with a bigger diameter being somewhat higher; however, as rebar corrosion progressed, the disparity substantially widened. It was also demonstrated that when structural degradation must be considered, bigger diameter rebar should be employed in structural design. Ductility is significantly degraded, especially for smaller reinforcement diameters (such as 8 mm). A considerable shift in the volumetric ratio between the microscopic layers is cited as the cause (martensite, bainite, pearlite). Other investigations came to the conclusion that there was no significant difference in the tensile characteristics of the various-sized naturally or artificially corroded bars. However, when naturally occurring and artificially created bars were compared, there were noticeable changes (Zhang et al. 2014; Imperatore et al. 2017).
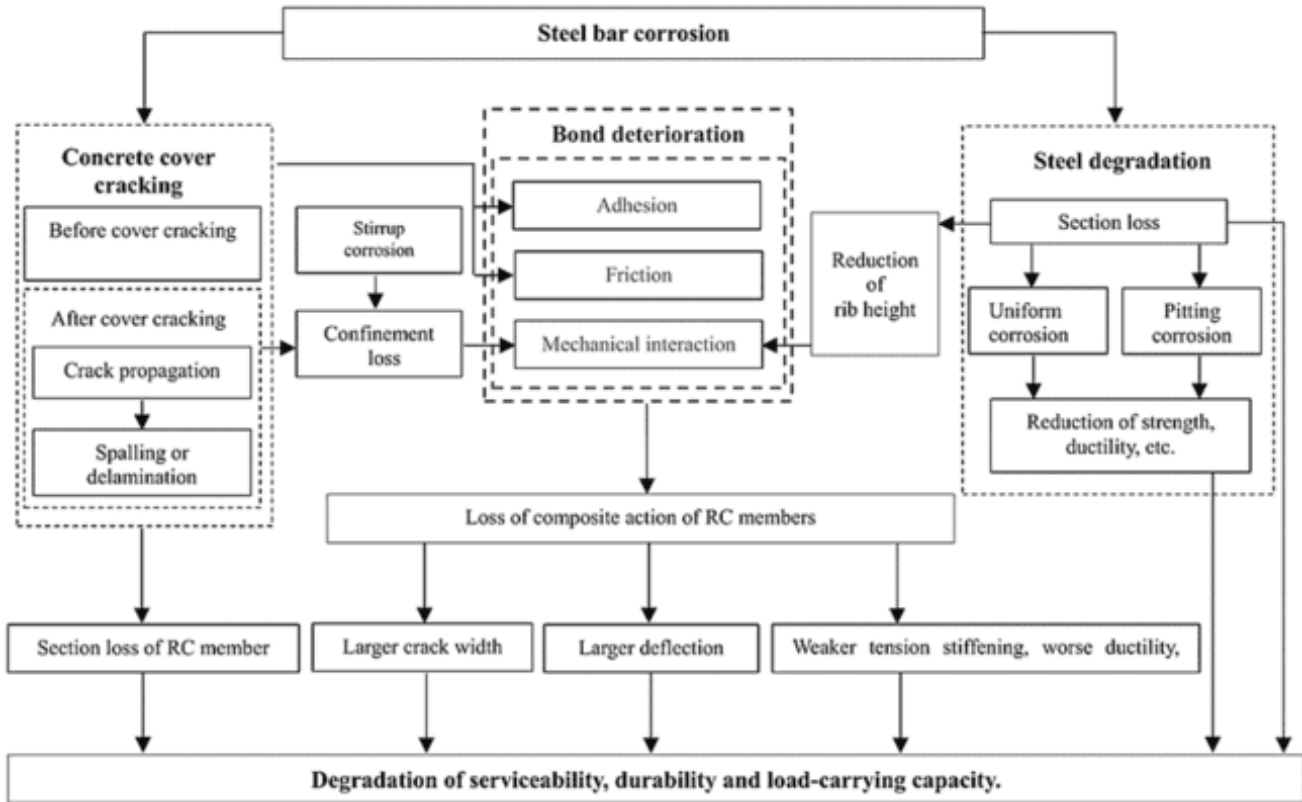
Fig.7. Influence of corrosion on bond deterioration, and its effects on structural and mechanical properties (Lin et al. 2019).

Since the uniform corrosion affects the entire length of the reinforcement, it exhibits lower penetration depth values than pitting corrosion but greater weight loss. Due to the localized character of the corrosive attack, (pits) are holes in the surface of the steel, are a common form in which the degradation tends to manifest itself. Pitting corrosion is an especially extreme form of corrosion since the cross-section is significantly reduced despite a very minor weight drop. As a result, the weight loss experienced by the bars throughout the corrosive process ought not be equated with the intensity of the corrosive attack. Since reinforcing corrosion is mostly a stochastic process, recent investigations have been implemented in order to evaluate the spatial variability of pitting corrosion with probabilistic models (Finozzi et al., 2018).
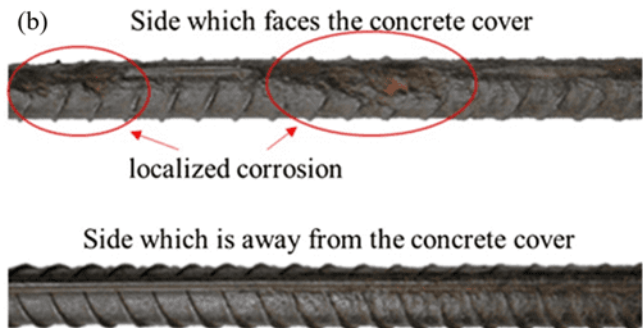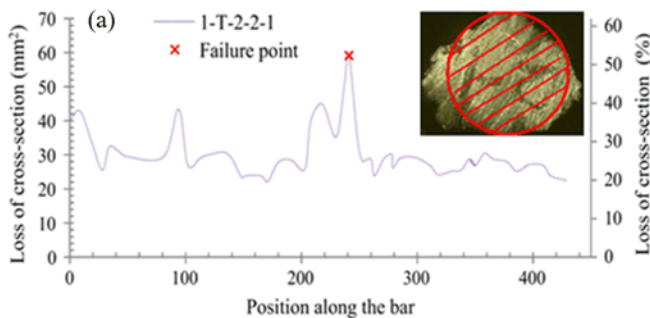

Fig.8. (a) Corrosion distributions of steel reinforcement, typical cross-section of the corroded steel reinforcement (Zhu et al. 2017), (b) a localized corrosion of the bar sides which, faces and away from the concrete cover (Xia et al. 2016).

The corrosion start time and corrosion rate for each spot on the surface of the rebar may differ, which causes the cross-sectional area of a corroded rebar to change along its length. As a result, the failure risk of corroded rebar rises in cross-sections that do not bear the maximum load. Because of the complicated form of the corrosion damage, identifying the exact cross-section at failure point is extremely difficult. Because the residual cross-section varied greatly around the disk, dispersion may appear as high as 20%. The lowest diameter measured with a Vernier caliper offers a conservative approximation of the cross-section. A length cut from the bar near the site of failure resulted in an

average cross section decrease, although the findings were influenced by dispersion (Francois et al. 2013). According to Zhu et al. (2017), the maximum cross-sectional loss might be as high as 53.1 %, while the specimens' average cross-sectional area losses ranged from 4.4 - 25.2%. Both along the longitudinal axis of the deteriorated steel reinforcement and around its periphery, the corrosion was randomly and unevenly distributed. The range of the specimens' gravimetric cross-sectional loss is between 0.9 and 41.1 % of the nominal cross-section. A typical deep pitting corrosion was represented by each peak of the curve in Fig 8. It is possible to ascertain that the bar 1T221's maximum cross-sectional loss is 59.25 mm^2, or around 52.4% of the initial nominal cross-section.

Reduction of strength and ductility

Corrosion severity has a substantial impact on steel's mechanical properties, particularly the maximum stress and strain. It's interesting to note that while the true ultimate strength among all the corroded steel bars has significantly increased, the true yield strength has remained almost constant. The main effect of corrosion that appeared to have an impact on standard compliance was a reduction in ultimate elongation. Making use of the actual cross-sectional area, it shown that the total elongation of the bars reduced but the ultimate tensile strength only slightly decreased as the degree of reinforcement corrosion lessen. Nominal elastic modulus and yield point decreased as reinforcement corrosion increased. Previous studies computed the stress of corroded steel bar from recorded force using the original cross-sectional area of the bar, the average decreased cross-sectional area of the bar, and the lowest cross-sectional area of the bar. Scholars dispute on which strategy is preferable than the others (Francois et al., 2013; Ou et al., 2016). Before proceeding, the nominal strength, which refers to the nominal cross-sectional area of the sound bar, as well as the effective strength, which refers to the residual cross-sectional area of the corroded bar, must be provided. Uniform and localized corrosion need to be differentiated for a greater comprehension of corrosion effects. The majority of researches agree on: reinforcing bar mechanical characteristics exposed to uniform corrosion remain unchanged. On the other hand, pitting corrosion is acknowledged as being more difficult to characterize in terms of the structural implications on reinforcing bars, and researchers are not always in agreement regarding these effects. The balance of mechanical properties is altered when a portion of the cross-section is lost, not only because of the reduction in section size but also because the external crowns of material that provide the outfit a higher load capacity are lost (Fernandez et al. 2015).

The elastic phase, yield plateau, strain hardening, and eventually the necking effect occur in the load-displacement relationship of non-corroded reinforcement. The corroded specimens, on the other hand, have a very distinct necking affect. Taking the rusted steel reinforcement as an example as Fig.9 illustrated that at the failure point, the non-corroded steel reinforcement underwent a necking action that clearly manifested as residual plastic deformation. Prior to yielding, the behavior of the corroded steel reinforcement is essentially identical to that of the uncorroded steel reinforcement; however, after yielding, there are varying degrees of shortening of the yield plateau stage, and no obvious necking phenomenon was seen during the tensile testing. Corroded steel reinforcement's brittle failure mode will gradually replace the ductile failure mode. One of the most essential characteristics stated for the reinforcement by design standards is that the steel reinforcement fails in the region with the highest corrosion degree, where there is strong pitting corrosion (Zhu et al. 2017). Whenever a locally thinned portion of a bar is subjected to tensile force (stretched) thus, stresses are focused at the notch, and the overall strain of the bar at failure is lower than that for an un-corroded bar. According to the study, while the total strain is only around 2.5 %, the damaged region has local strains of about 30 %. The tendency becomes more obvious as the testing progresses, and the pit's elongation can reach up to 63.2 % of the entire bar elongation (Finozzi et al. 2018).
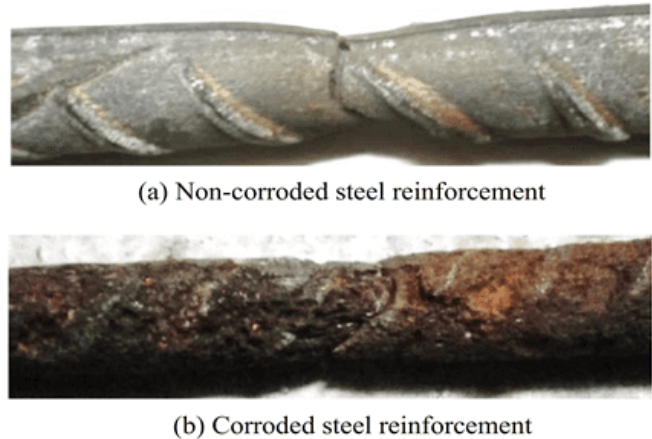

(a) Non-corroded steel reinforcement

(b) Corroded steel reinforcement

Fig.9. Failure points with different necking effect (Zhu et al., 2017).

FORMULATION OF CORROSION-MECHANICAL PROPERTIES

Formulas from previous studies

Before discussing the loss in the ductility and strength of the reinforcing bars, some important relationships have been provided in Eq.13–16, to calculate the rate of corrosion, the estimated mass loss in addition the average loss of cross-sectional area.

$$Corrosion\ rate\ (mm/yr) = (1000 \times M)/(A \times t \times \rho) \qquad (13)$$

Where:

M is the mass loss of the embedded steel bars in grams, ρ is the density of steel of 7.87 g/cm^3, A is the total surface area of the steel attacked by corrosion in mm^2, and t is the test duration in

years (Ma et al. 2015).

$$Avg.sec.loss\ ratio = [d^2 - (d - 2 \times 0.0116 \times t)^2]/d^2 \quad (14)$$

Where:

d is the initial nominal dia. of non-corroded bar in mm, t years since the corrosion initiation, (Zhang et al. 2014).

Through literatures the amount of structural damage caused by chloride-induced corrosion determined by applying Faraday's Law, which relates the current flowing during the electrochemical reaction to the mass of steel consumed during the corrosion process.

$$M = (m \times I \times t)/(z \times F) \quad (15)$$

Where:

M is the mass loss (g), m here is the atomic mass of iron (56 g for Fe), F is Faraday's constant (96500 A·s), z is the ionic charge (for instance, 2 for Fe→Fe^{2+}+2e$^-$), t is the time after corrosion initiation (s), and I is the current (A), (I = a$_s$× i$_{corr}$), a$_s$ is the surface area of rebar (cm^2), i$_{corr}$ is the current density (A/cm^2)]. For a unit length of the rebar, a$_s$ = πd. Thus, the mass loss per unit length for a time step after corrosion initiation, Δt (s), is as in Eq.16, where, d^r is the residual rebar diameter (Cui. 2016).

$$M = 2.894 \times 10^{-4} \times i_{corr} \times \pi \times d^r \times \Delta t \quad (16)$$

The general form used in most studies on the corrosion of reinforcing bars are similar to those shown in Eq.17–20. Linear relationship for yield strength and ultimate strength is determined by most researchers, however, some studies provided an exponential equation for elongation to describe scattered data points.

$$F_{yC} = (1 - \alpha_y M) \cdot F_y \quad (17)$$

$$F_{uC} = (1 - \alpha_u M) \cdot F_u \quad (18)$$

$$\varepsilon_{uC} = (1 - \alpha_e M) \cdot \varepsilon_u \quad (19)$$

$$\varepsilon_{uC} = (e^{a \cdot M}) \cdot \varepsilon_u \quad (20)$$

Where:

F$_{yc}$, F$_{uc}$, ε$_{uC}$, F$_y$, F$_u$, ε$_u$ are yield strength, ultimate strength and elongation of corroded and un-corroded bars, respectively, M is the average mass loss (%), α$_y$, α$_u$, α$_e$ are the reduction factors for yield strength, ultimate strength, and elongation, respectively, and a is a statistical coefficient in the exponential equation.

Table 3 lists the reduction factors discovered via earlier research by other authors for tensile behavior for naturally as well as artificially corroded steel bars. Due to the fact that bar size and type (such as plain rounded bars or deformed bars) had little to no impact on the reduction factors, they were neglected in the comparison. There is not a significant difference between the reduction factors for elongation and final strain, despite the fact that many reduction factors were calculated using a collection of bars of various diameters. The yield stress, ultimate stress, as well as ultimate strain or elongation reduction factors of a naturally corroded steel bars were (0.007-0.030, 0.009-0.028, 0.013-0.060, respectively) and are typically higher than those for carbonation corrosion (0.010-0.011, 0.011-0.014, 0.014-0.018, respectively). This supports the widespread notion in the literature that chloride attack encourages much non-uniform corrosion than carbonation. For steel bars that had been intentionally corroded, the impressed-current (or electrical) approach, to perform the artificial corrosion on bars that are embedded in concrete or on bare bars, a cyclical technique that comprised wetting and drying concrete specimens cast with salt, or salt spray, was utilized. The impressed-current approach's reduction factors for each of yield stress, ultimate stress, as well as ultimate strain or elongation for bars immersed in concrete were 0.011-0.024, 0.011-0.021, 0.020-0.052, and 0.012-0.016, 0.012-0.017, 0.017-0.034, respectively. Because corroded embedded bars lost more yield stress and elongation than corroded bare bars.

The reduction factors for concrete-immersed bars are the same as or greater than those for exposed bars. Surprisingly, the impressed-current technique is more suited to altering corrosion induced by chloride attack on concrete-immersed bars than bare bars. This is performed by comparing the reduction factor values obtained by the impressed-current approach with those obtained via spontaneous corrosion. Reduction factors from buried bars are mainly closer to the top limit of allowable chloride attack reduction factors than reduction factors from bare bars. On bare bars, the impressed-current method's reduction factors resemble those of carbonation corrosion in general (Ou et al. 2016; Imperatore et al. 2017).

Proposed formulas for estimation of residual mechanical properties

Numerous experimental datasets on corrosion of steel rebar that consists of 443 datasets, from 12 studies (Almusallam, 2001; Apostolopoulos & Papadakis, 2008; Apostolopoulos et al., 2013; Francois et al., 2013; Huang, 2014; Fernandez et al. 2015; Ou et al., 2016; Lu et al., 2016; Imperatore et al., 2017; Zhu et al., 2017; Fernandez & Berrocal, 2019; Ahmed, 2022) have been sorted out and, accordingly, analyzed statistically. Analyzing the obtained results, steel mechanical property degradation equations are defined in accordance with these equations based on statistical methods. Linear and exponential regression best suit the yielding as well as ultimate stresses, in addition the ultimate strain. The coefficients of the ordinary least squares' technique are used to

create linear regression equations. The sum of the squares of the residuals is lowered to match a nearly continuous function. The sum of the squares of the residuals is then decreased, in addition the decay laws of yielding as well as ultimate stresses for the non-dimensional stresses shown at ordinate in addition to the percentage of mass loss shown at abscissa explained (Fig.10). Reduction factors were determined to set a relationship of

tensile behaviors within the average loss of mass regarding both naturally as well as artificially corroded bars. Tensile stresses are determined by a simple division technique (recoded load in the numerator and the corresponding corroded average cross-sectional area of rebar in the denominator), this is denoted by an observed generalized corrosion degree.

Table 3 Reduction factors proposed in previous studies

Author	Data type	αy	αu	αe	a
Cairns et al. 2005	Artificial corrosion, machined pits	0.012	0.011	0.030	
Tang et al. 2014	Accelerated corrosion- based on average mass loss	0.017	0.017		
	Accelerated corrosion – based on critical area	0.009	0.009		
Ou et al. 2016	Experimental data, bars subjected to natural corrosion	0.012	0.012	0.013	
	Experimental data bars subjected to artificial accelerated corrosion	0.013	0.012	0.028	
Cui, 2016	Experimental data bars subjected to artificial accelerated corrosion	0.015	0.015	0.039	
Lu et al. 2016	Natural & artificial exposure, uniform corrosion	0.020	0.023		
	Natural & artificial exposure, pitting corrosion	0.030	0.035		
Imperatore et al. 2017	Experimental data by the authors accelerated corrosion	0.015	0.014		– 0.028
	Collected from literature-uniform corrosion	0.014	0.013		– 0.020
	Collected from literature-pitting corrosion	0.020	0.019		– 0.055
Finozzi et al. 2018	Experimental data for machined (artificial) pits	0.013	0.018		– 0.041
Sun et al. 2018	Experimental data, artificial corrosion –average loss of area	0.011	0.013		
	Experimental data, artificial corrosion –critical loss of area	0.006	0.007		
Fernandez & Berrocal, 2019	Experimental data, natural corrosion	0.014	0.014		
Ahmed, 2022	Experimental data, bars subjected to natural corrosion	0.018	0.020	0.026	

As a result, the degree of corrosion was treated as a specimen global variable (generalized corrosion) rather than the particular corrosion degree of the critical cross-section, which consistently demonstrated a greater mass loss owing to the critical pit. When the generalized corroded cross-section area hypothesis is used, the effective stress or modulus values are lower than when the genuine cross-section diameter hypothesis is used. Despite the scatter data precluding any reliable association with the corrosion degree, the effect of corrosion on rebar ductility results in a non-linear action, which is also more dangerous than anticipated. The decay equations for each scenario are constructed, and the associated R^2 coefficient calculated. This parameter indicates the percentage of the dependent variable's spread that the independent variable can predict. The R^2 coefficient may be used to assess the accuracy of the regression.

Fig.10 describes the variation of the yielding and the maximum strength of corroded bars in comparison with those of uncorroded steel for the various measured degrees of corrosion. As anticipated, the capacity reduction reduced linearly as the degree of corrosion increased. The reduction factors in Eqs.21–24 illustrate how the amount of corrosion mass loss affects the tensile behavior and ductility of reinforcing bars. The yield stress as well as ultimate stress reduction factors were more than 0.01, It implies that stresses diminishing to zero for certain rate

of corrosion mass loss less than 80%. The scattered data for the link between elongation and mass loss may be relevant to variations in the volumetric ratio amid all microstructural layers as well as localized reductions in the cross section of the reinforcement.

$$F_{yC} = (1 - 0.0134M) \cdot F_y \qquad (21)$$

$$F_{uC} = (1 - 0.0130M) \cdot F_u \qquad (22)$$

$$\varepsilon_{uC} = (1 - 0.0209M) \cdot \varepsilon_u \qquad (23)$$

$$\varepsilon_{uC} = (e^{-0.036 \cdot M}) \cdot \varepsilon_u \qquad (24)$$

SUMMARY AND CONCLUDING REMARKS

Corrosion of reinforcing steel rebar must be regarded in particular most prevalent and fundamental reason for degradation observed in reinforced concrete structures that are already exists. Corrosion leads to expansive pressure, results in internal cracking and, lastly, spalling and delamination, or even collapse of the structures. Corrosion linked with maintenance/repair according to reports; global RC infrastructure costs roughly $100 billion per year. Understanding the corrosion mechanism,

corrosion types, and the corrosion influence on the construction projects could lead to the reduction of the severe structural failures and damages coming in that way. Therefore, the research related to corrosion of the concrete reinforcing bars is still needed, since it can
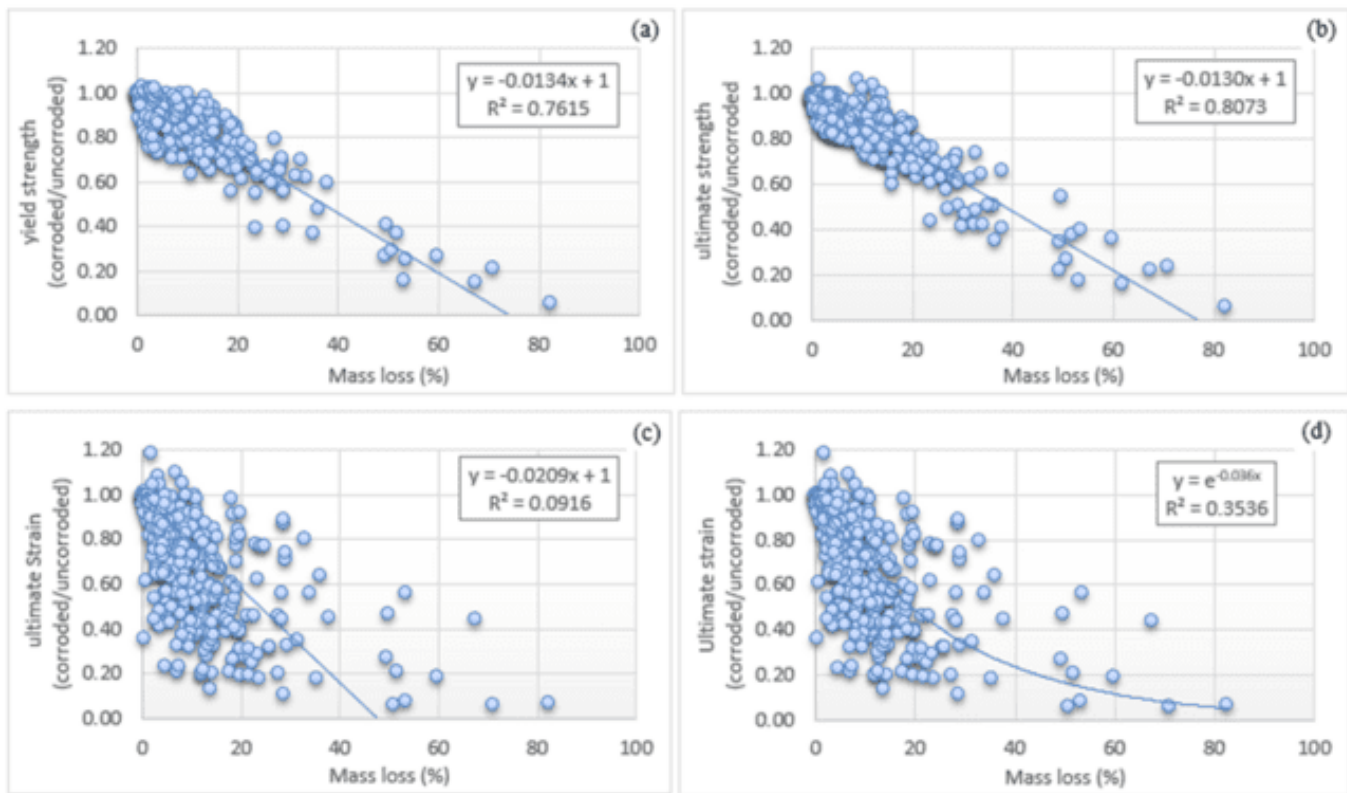

Fig.10. Relation between the average mass loss and the mechanical properties of the corroded/un-corroded rebar, (a) yield strength, (b) ultimate strength, (c) ultimate strain-linear, and (d) ultimate strain-exponential.

save billions in the budget of the construction projects worldwide, and can help the engineers to be more precise in considering corrosion consequences. Regarding this study, degradation equations for the mechanical properties of rebar owing to corrosion have been defined. Achieved results showed that yield strength, ultimate strength in addition, rebar ductility decreases as the corrosion damage for all bar diameters increases. It has been determined that only taking uniform corrosion into account could result in an overestimation of the structure's remaining capacity for carrying loads. For a more accurate computation, both corrosion impacts must be considered. The two key variables were the diversity of pitting corrosion in terms of where and when it occurs, as well as the reduction in ductility of the corroded reinforcing bar. The proposed formulas can be used for deformed reinforcing bars ranging Ø8-25 mm, corroded naturally or artificially, embedded in concrete or bare bars. The loss of strength (yield and ultimate) was found to have a linear relationship with the degree of corrosion, and the results' scatter was within the range expected for samples that weren't rusted. There are two established correlations between the average mass loss and the remaining ultimate strain. The exponential relationship appears to be more precise than the linear relationship. The mass loss of 1% due to the rebar corrosion can cause the strength loss of 1.34% and 1.30%, respectively for yield and ultimate strength; and an elongation loss of 2.09% and 3.54% for linear and exponential equations, respectively.

REFERENCES

Abdelatif A.O., Ozbolt J., Gambarelli S., 3D finite element modelling of corrosion of lap splice joints in concrete, Construction and Building Materials 169 (2018) 124–131.

Ahmad S., Reinforcement corrosion in concrete structures, its monitoring and service life prediction—a review, Cement & Concrete Composites 25 (2003) 459–471.

Ahmed G.H., Askandar N.H., Jumaa G.B., A review of largescale 3DCP: Material characteristics, mix design, printing process, and reinforcement strategies, Structures 43 (2022) 508–532.

Ahmed G.H., Influence of time dependent corrosion on strength and ductility of reinforcing steel bars exposed to natural and aggressive environments, Polytechnic Journal. 2022. 12(1).

Ahmed G.H., Mechanical properties of welded deformed reinforcing steel bars, ARO, The Scientific Journal of Koya University, V(3), No.1(2015), 28–39, http://dx.doi.org/10.14500/aro.10059 .

Almusallam A.A., Effect of degree of corrosion on the properties of reinforcing steel bars, Construction and Building Materials 15 (2001) 361-368.

Apostolopoulos C.A., Demis S., Papadakis V.G., Chloride-induced corrosion of steel reinforcement – Mechanical performance and pit depth analysis, Construction and Building Materials 38 (2013) 139–146.

Apostolopoulos C.A., Papadakis V.G., Consequences of steel corrosion on the ductility properties of reinforcement bar, Construction and Building Materials 22 (2008) 2316–2324.

Balestra C.E.T., Lima M.G., Silva A.R., Junior R.A.M., Corrosion degree effect on nominal and effective strengths of naturally corroded reinforcement, J. Mater. Civ. Eng. (2016), 04016103.

Balestra C.E.T., Nakano A.Y., Savaris G., Junior R.A.M., Reinforcement corrosion risk of marine concrete structures evaluated through electrical resistivity: Proposal of parameters based on field structures, Ocean Engineering 187 (2019) 106167.

Bautista A., Pomares J.C., Gonzalez M.N., Velasco F., Influence of the microstructure of TMT reinforcing bars on their corrosion behavior in concrete with chlorides, Construction and Building Materials 229 (2019) 116899.

Bazan A.M., Galvez J.C., Reyes E., Lamuela D.G., Study of the rust penetration and circumferential stresses in reinforced concrete at early stages of an accelerated corrosion test by means of combined SEM, EDS and strain gauges, Construction and Building Materials 184 (2018) 655–667.

Brito JD, Kurda R., The past and future of sustainable concrete: A critical review and new strategies on cement-based materials, Journal of Cleaner Production, 2021, 281(8):123558.

Cairns J., Plizzari G.A., Du Y., Law D.W., Franzoni C., Mechanical properties of corrosion-damaged reinforcement, ACI materials journal, Title no. 102-M29, 102(4) Jul/Aug (2005), 256 – 264.

Chen D., Mahadevan S., Chloride-induced reinforcement corrosion and concrete cracking simulation, Cement & Conc. Composites 30 (2008) 227–238.

Chen F.X., Zhong Y.C., Gao X.Y., Jin Z.Q, Wang E.D., Zhu F.P., Shao X.X., He X.Y., Non-uniform model of relationship between surface strain and rust expansion force of reinforced concrete, Scientific Reports, (2021) 11:8741, nature portfolio, https://doi.org/10.1038/s41598-021-88146-2.

Cui Z., Lifetime performance prediction of reinforced concrete structures in multi-threat areas, Graduate Theses and Dissertations, 15285, PhD dissertation, Iowa State University, 2016, 188 pages, https://lib.dr.iastate.edu/etd/15285.

Diaz B., Guitian B., Novoa X.R., Perez M.C., The effect of chlorides on the corrosion behavior of weathered reinforcing bars, Electrochimica Acta 336 (2020) 135737.

Eid J., Takenouti H., Saadi B.A., Taibi S., Electrochemical studies of steel rebar corrosion in clay: Application to a raw earth concrete, Corrosion Science (2020), V.168, 15 May 2020, 108556, https://doi.org/10.1016/j.corsci.2020.108556 .

Fernandez I., Bairan J.M., Mari A.R., Corrosion effects on the mechanical properties of reinforcing steel bars. Fatigue and σ–ε behavior, Construction and Building Materials 101 (2015) 772–783.

Fernandez I., Berrocal C.G., Mechanical Properties of 30 Year-Old Naturally Corroded Steel Reinforcing Bars, International Journal of Concrete Structures and Materials, (2019) 13:9, https://doi.org/10.1186/s40069-018-0308-x .

Finozzi I., Saetta A., Budelmann H., Structural response of reinforcing bars affected by pitting corrosion: experimental evaluation, Construction and Building Materials 192 (2018) 478–488.

Firodiya P.K., Sengupta A.K., Pillai R.G., Evaluation of Corrosion Rates of Reinforcing Bars for Probabilistic Assessment of Existing Road Bridge Girders, J. Perform. Constr. Facil. (2015), 04014067, https://doi.org/10.1061/(ASCE)CF.1943-5509.0000579 .

Francois R., Khan I., Dang V.H., Impact of corrosion on mechanical properties of steel embedded in 27-year-old corroded reinforced concrete beams, Materials and Structures (2013) 46:899–910.

Gao Y., Zheng Y., Zhang J., Xu S., Zhou X., Zhang Y., Time-dependent corrosion process and non-uniform corrosion of reinforcement in RC flexural members in a tidal environment, Construction and Building Materials 213 (2019) 79–90.

Garcia D., Laurens S., Panin S., A comprehensive study of the spatial distribution of the galvanic protection current supplied by zinc layer anodes applied to steel-reinforced concrete structures, Corrosion Science 158 (2019) 108108.

Garcia E., Torres J., Rebolledo N., Arrabal R., Sanchez J., Corrosion of steel rebars in anoxic environments. Part I:

83

Electrochemical measurements, MDPI, Materials 2021, 14, 2491. https://doi.org/10.3390/ma14102491 .

Ghafur H. Ahmed, Omar Q. Aziz, Shear behavior of dry and epoxied joints in precast concrete segmental box girder bridges under direct shear loading, Engineering Structures 182 (2019) 89–100.

Hu J., Deng P., Li X., Zhang J., Wang G., the vertical Non-uniform corrosion of Reinforced concrete exposed to the marine environments, Construction and Building Materials 183 (2018) 180–188.

Hu M., Han Q., Xu K., Du X., Corrosion influences on monotonic properties of ultra-high-strength reinforcing steels, Construction and Building Materials 198 (2019) 82–97.

Huang C.H., Effects of rust and scale of reinforcing bars on the bond performance of reinforcement concrete, J. Mater. Civ. Eng., 2014, 26(4): 576-581.

Imperatore S., Rinaldi Z., Drago C., Degradation relationships for the mechanical properties of corroded steel rebars, Construction and Building Materials 148 (2017) 219–230.

Jiang B., Doi K., Tsuchiya K., Kawano Y., Kori A., Ikushima K., Micromechanical properties of steel corrosion products in concrete studied by Nano-indentation technique, Corrosion Science (2019), V.163, Feb. 2020, 108304, https://doi.org/10.1016/j.corsci.2019.108304 .

Jones S., Martys N., Lu Y., Bentz D., Simulation studies of methods to delay corrosion and increase service life for cracked concrete exposed to chlorides, Cement & Concrete Composites 58 (2015) 59–69.

Koulouris K., Apostolopoulos C., Study of the residual bond strength between corroded steel bars and concrete—A Comparison with the recommendations of Fib Model Code 2010, MDPI, Metals 2021, 11, 757, https://doi.org /10.3390/met11050757 .

Lin H., Zhao Y., Feng P., Ye H., Ozbolt J., Jiang C., Yang J.Q., State-of-the-art review on the bond properties of corroded reinforcing steel bar, Construction and Building Materials 213 (2019) 216–233.

Lin H., Zhao Y., Ozbolt J., Wolf R. H., Bond strength evaluation of corroded steel bars via the surface crack width induced by reinforcement corrosion, Engineering Structures 152 (2017) 506–522.

Lu C., Yuan S., Cheng P., Liu R., Mechanical properties of corroded steel bars in pre-cracked concrete suffering from chloride attack, Construction and Building Materials 123 (2016) 649–660.

Ma Q., Nanukuttan S.V., Basheer P.A.M., Bai Y., Yang C., Chloride transport and the resulting corrosion of steel bars in alkali activated slag concretes, Materials and Structures, 2015, https://doi.org/10.1617/S11527-015-0747-7 .

Michel A., Otieno M., Stang H., Geiker M.R., Propagation of steel corrosion in concrete: Experimental and numerical investigations, Cement and Concrete Composites 70 (2016) 171-182.

Ou Y.C., Susanto Y.T.T., Roh H., Tensile behavior of naturally and artificially corroded steel bars, Const. and Building Materials 103 (2016) 93–104.

Shekhar S., Ghosh J., Padgett J.E., Seismic life-cycle cost analysis of ageing highway bridges under chloride exposure conditions: modelling and recommendations, Structure and Infrastructure Engineering, 14:7 (2018), 941-966, https://doi.org/10.1080/15732479.2018. 1437639.

Sola E., Ozbolta J., Balabanic G., Mir Z.M., Experimental and numerical study of accelerated corrosion of steel reinforcement in concrete:

Transport of corrosion products, Cem Conc Research 120 (2019) 119–131.

Soleimani M., Mirzadeh H., Dehghanian C., Effects of tempering on the mechanical and corrosion properties of dual phase steel, Materials today communications, V.22, March 2020, 100745, https://doi.org/10.1016/j. mtcomm.2019.100745

Sun X., Kong H., Wang H., Zhang Z., Evaluation of corrosion characteristics and corrosion effects on the mechanical properties of reinforcing steel bars based on three-dimensional scanning, Corrosion Science (2018), V.142, Sep. 2018, 284 – 294, https://doi.org/10.1016/j.corsci.2018.07.030 .

Tang F., Corrosion of steel fibre reinforced concrete (SFRC) subjected to simulated stray direct (DC) interference, Mat. Today Com. 20 (2019) 100564.

Tang F., Lin Z., Chen G., Yi W., Three-dimensional corrosion pit measurement and statistical mechanical degradation analysis of deformed steel bars subjected to accelerated corrosion, Con. and Building Materials 70 (2014) 104–117.

Uthaman S., George R.P., Vishwakarma V., Harilal M., Philip J., Enhanced seawater corrosion resistance of reinforcement in nanophase modified fly ash concrete, Construction and Building Materials 221 (2019) 232–243.

Uygunogu T., Gunes I., Biogenic corrosion on ribbed reinforcing steel bars with different bending angles in sewage systems, Construction and Building Materials 96 (2015) 530–540.

Wang X., Nguyen M., Stewart M.G., Syme M., Leitch A., Analysis of climate change impacts on the deterioration of concrete infrastructure–Part 1: Mechanisms, practices, modelling and simulations–A review, published by CSIRO, Canberra, (2010), ISBN 9780 4310365 8.

Xia J., Jin W.L., Li L.Y., Performance of corroded reinforced concrete columns under the action of eccentric loads, Journal of Materials in Civil Engineering, Vol 28, No 1, Jan. 2016, https://doi.org/ 10.1061/(ASCE)MT.1943-5533.0001352

Xu Y., Jin R., Measurement of reinforcement corrosion in concrete adopting ultrasonic tests and artificial neural network, Construction and Building Materials 177 (2018) 125–133.

Yuan Y., Ji Y., Jiang J., Effect of corrosion layer of steel bar in concrete on time-variant corrosion rate, Materials and Structures (2009) 42:1443–1450, https://doi.org/10. 1617/s11527-008-9464-9 .

Zhang W., Francois R., Yu L., Influence of load-induced cracks coupled or not with top-casting-induced defects on the corrosion of the longitudinal tensile reinforcement of naturally corroded beams exposed to chloride environment under sustained loading, Cement and Conc. R. 129 (2020) 105972.

Zhang W., Zhou B., Gu X., Dai H., Probability Distribution Model for Cross-Sectional Area of Corroded Reinforcing Steel Bars, J. Mater. Civ. Eng., 2014, 26(5): 822-832.

Zhang X., Li B., Shear-strength capacity assessment of corroded reinforced concrete beam-column joints, J. Perform. Constr. Facil., 2018, 32(5): 04018067.

Zhu W., Francois R., Poon C.S., Dai J.G., Influences of corrosion degree and corrosion morphology on the ductility of steel reinforcement, Construction and Building Materials 148 (2017) 297–306.